Published in final edited form as:
*J Am Chem Soc*. 2013 February 13; 135(6): . doi:10.1021/ja3117203.

# Mechanism of Copper(I)/TEMPO-Catalyzed Aerobic Alcohol Oxidation

**Jessica M. Hoover**[†], **Bradford L. Ryland**, and **Shannon S. Stahl**[*]
Department of Chemistry, University of Wisconsin—Madison, 1101 University Avenue, Madison, Wisconsin 53706, United States

## Abstract

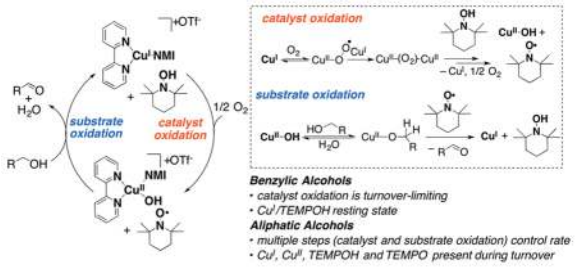


Homogeneous Cu/TEMPO catalyst systems (TEMPO = 2,2,6,6-tetramethylpiperidine-*N*-oxyl) have emerged as some of the most versatile and practical catalysts for aerobic alcohol oxidation. Recently, we disclosed a (bpy)$Cu^{I}$/TEMPO/NMI catalyst system (NMI = *N*-methylimidazole) that exhibits fast rates and high selectivities, even with unactivated aliphatic alcohols. Here, we present a mechanistic investigation of this catalyst system, in which we compare the reactivity of benzylic and aliphatic alcohols. This work includes analysis of catalytic rates by gas-uptake and in situ IR kinetic methods and characterization of the catalyst speciation during the reaction by EPR and UV–visible spectroscopic methods. The data support a two-stage catalytic mechanism consisting of (1) "catalyst oxidation" in which $Cu^{I}$ and TEMPO–H are oxidized by $O_2$ via a binuclear $Cu_2O_2$ intermediate and (2) "substrate oxidation" mediated by $Cu^{II}$ and the nitroxyl radical of TEMPO via a $Cu^{II}$-alkoxide intermediate. Catalytic rate laws, kinetic isotope effects, and spectroscopic data show that reactions of benzylic and aliphatic alcohols have different turnover-limiting steps. Catalyst oxidation by $O_2$ is turnover limiting with benzylic alcohols, while numerous steps contribute to the turnover rate in the oxidation of aliphatic alcohols.

## INTRODUCTION

The oxidation of alcohols to aldehydes, ketones and carboxylic acids is perhaps the most widely used class of oxidation reactions in organic chemistry. Many reagents and catalysts exist for these transformations,[1] but the development of practical aerobic oxidation methods remains a challenge.[2] Extensive attention has focused on homogeneous $Pd^{II}$ catalysts for aerobic alcohol oxidation,[3,4] but a recent effort to use $Pd^{II}$ catalysts in a scalable, flow



Corresponding Author: stahl@chem.wisc.edu.
[†]**Present Address:** C. Eugene Bennett Department of Chemistry. West Virginia University, P.O. Box 6045, Morgantown, WV 26506

The authors declare no competing financial interest.

Supporting Information
Detailed experimental procedures, kinetic data, and additional experiment data are included. This material is available free of charge via the Internet at http://pubs.acs.org.

method suitable for pharmaceutical process chemistry highlighted a number of limitations of these catalysts.[5] Problematic issues include the tendency of $Pd^{II}$ to decompose under the reaction conditions into inactive Pd black, inhibition of the catalyst by heterocycles and other coordinating functional groups, and relatively slow catalytic turnover rates that decrease the practicality of these methods. In addition, primary aliphatic alcohols are difficult substrates because even a small amount of overoxidation to the carboxylic acid can lead to poisoning of the $Pd^{II}$ catalyst.[3a]

We recently reported a (bpy)$Cu^{I}$/TEMPO catalyst system with NMI (bpy =2,2 □bipyridine, TEMPO = 2,2,6,6-tetrame-thylpiperidine-*N*-oxyl, NMI = *N*-methylimidazole) that overcomes nearly all of the limitations associated with $Pd^{II}$ catalysts (Chart 1).[6] This catalyst system enables chemoselective oxidation of benzylic, allylic and aliphatic primary alcohols to the corresponding aldehydes, with rates at least an order of magnitude higher than those observed with $Pd^{II}$ catalysts. Moreover, the method is compatible with substrates bearing diverse functional groups and uses ambient air as the source of the $O_2$ oxidant.

Homogeneous Cu/nitroxyl-radical catalysts for aerobic alcohol oxidation were identified nearly 50 years ago when Brackman and Gaasbeek reported the oxidation of methanol with a (phenanthroline)$Cu^{II}$/di-*tert*-butylnitroxyl cocatalyst system.[7] These results received little subsequent attention, however. In 1984, Semmelhack and co-workers demonstrated aerobic oxidation of benzylic and allylic alcohols with 10% CuCl/TEMPO in DMF as the solvent.[8] Aliphatic alcohols proved to be substantially less reactive and required 2 equiv of $CuCl_2$ to achieve good product yields.

Subsequent work highlighted the beneficial effect of chelating nitrogen ligands for Cu, and more than a dozen catalyst systems of this type have been reported.[9,10] Notable examples include a (bpy)$CuBr_2$/TEMPO catalyst system that employs *t*BuOK as a catalytic base in $CH_3CN/H_2O$ as the solvent, developed by Sheldon and co-workers,[9d, e] and a (bpy)$Cu(OTf)_2$/TEMPO catalyst system reported by Kumpulainen and Koskinen.[9m] In our work, we observed a significant rate enhancement by replacing $Cu^{II}$ with a $Cu^{I}$ source, and the catalyst system in Chart 1 is notable for its efficiency in the oxidation of aliphatic alcohols.

Similar Cu/nitroxyl-radical catalyst systems have been reported very recently for a number of other aerobic oxidation reactions.[11] Examples include the oxidation of amines to imines, the oxidative coupling of alcohols and amines, and oxidative dehydrogenation routes to aromatic heterocycles.

The growing synthetic utility and significance of the Cu/ TEMPO-catalyzed reactions prompted us to undertake a thorough mechanistic study of (bpy)$Cu^{I}$/TEMPO-catalyzed aerobic alcohol oxidation.[12] In the literature, Cu/TEMPO catalyst systems are frequently compared to galactose oxidase,[13] an enzyme that mediates aerobic alcohol oxidation at a mononuclear Cu center with a redox active phenolate/phenoxyl radical ligand.[14–16] On the other hand, TEMPO-catalyzed oxidations of alcohols with a variety of stoichiometric oxidants often proceed via an oxoammonium cation intermediate ($TEMPO^{+}$),[17] and alcohol oxidation by oxoammonium reagents is well-known.[18] Studies probing the galactose oxidase and oxoammonium pathways with the (bpy)$Cu^{I}$/TEMPO catalyst system are described below.

In addition, systematic kinetic and spectroscopic studies of (bpy)$Cu^{I}$/TEMPO-catalyzed alcohol oxidation are presented. The data provide the basis for a catalytic mechanism that features two separate half-reactions: (1) oxidation of $Cu^{I}$ and TEMPOH by $O_2$ and (2) alcohol oxidation by $Cu^{II}$ and TEMPO. Significant mechanistic differences are observed between the reactions of benzylic and aliphatic alcohols. For example, the catalytic rate

laws, identities of the catalyst resting states, and kinetic isotope effects differ for the two substrates. The data obtained with the two substrates provide substantial insights into the fundamental steps associated with the two catalytic half-reactions, and they explain the historical difficulty in achieving efficient oxidation of aliphatic alcohols. Overall, this study provides a valuable foundation for ongoing efforts to expand the scope of aerobic oxidation reactions and the development of transition-metal catalysts that employ redox-active organic cocatalysts.

## RESULTS AND DISCUSSION

### Qualitative Mechanistic Observations

In light of the unique efficiency of the (bpy)$Cu^{I}$/TEMPO catalyst system in the oxidation of aliphatic primary alcohols, we elected to perform independent mechanistic studies of the oxidation of benzyl alcohol ($PhCH_2OH$) and cyclohexylmethanol (Cy-$CH_2OH$) as representative activated and unactivated substrates (eq 1). The "(bpy)$Cu^{I}$/TEMPO" catalyst system employed here consists of 5 mol % $[Cu(MeCN)_4](OTf)$, 5 mol % bpy, 5 mol % TEMPO, and 10 mol % NMI in MeCN.

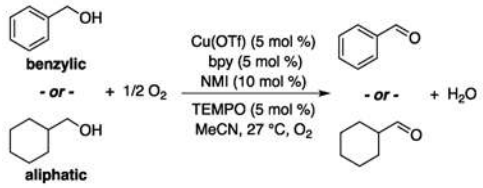


(1)

(bpy)$Cu^{I}$/TEMPO-catalyzed oxidation of benzylic alcohols is rapid; complete conversion of $PhCH_2OH$ is achieved in ~30 min at room temperature with ambient air as the oxidant. The oxidation of aliphatic alcohols is slower, often requiring 20–24 h to reach completion under comparable conditions. The progress of the reactions in eq 1 was readily followed by in situ IR spectroscopy, monitoring formation of the aldehyde, and by gas-uptake methods, monitoring consumption of $O_2$ within a sealed reaction vessel (Figure 1).

Quantitation of $O_2$ consumption and aldehyde formation reveals an $O_2$:$RCH_2OH$ stoichiometry of ~0.5 for both alcohol substrates, indicating that $O_2$ is converted completely to $H_2O$, as shown in eq 1. This result differs from some other Cu-catalyzed aerobic alcohol oxidations that form hydrogen peroxide and exhibit an $O_2$:$RCH_2OH$ stoichiometry of ~1.0.[16] Control experiments show that $H_2O_2$ disproportionates rapidly under the (bpy)$Cu^{I}$/TEMPO catalytic reaction conditions (eq 2, Supporting Information Figure S1). This result indicates that $H_2O_2$ is not a viable oxidant for these reactions and would not accumulate, if formed as a byproduct of the reaction.

$$H_2O_2 \xrightarrow{(bpy)Cu^{I}/TEMPO} H_2O + 1/2\, O_2 \quad (2)$$

During the oxidation of $PhCH_2OH$, the reaction mixture has a dark red-brown color. The color changes rapidly to green upon complete consumption of alcohol. Addition of another 20 equiv of $PhCH_2OH$ to this reaction mixture results in a rapid change of the color back to red-brown until the second aliquot of $PhCH_2OH$ is fully converted to benzaldehyde, as determined by in situ IR spectroscopy (Figure 2).

The red-brown color observed during the catalytic reaction matches that of an anaerobic solution of $Cu^{I}(OTf)$, bpy, and NMI in acetonitrile, and the green color observed at the end of the reaction is consistent with the formation of bpy-ligated $Cu^{II}$ species (see below for further details).

Stoichiometric experiments performed under $N_2$ show that bpy, $Cu^{II}$ and TEMPO can mediate kinetically competent oxidation of the alcohol, even in the absence of $O_2$, provided a strong base is present.[19] TEMPO is required for the reaction. For example, when a 1:1 bpy/$Cu^{II}(OTf)_2$ solution was added to 4 equiv of $PhCH_2OH$ under $N_2$, no benzaldehyde was detected by in situ IR spectroscopy; however, aldehyde formed rapidly upon addition of TEMPO (Supporting Information Figure S2). Catalytic turnover ensued upon exposure of this solution to an atmosphere of $O_2$. The rate of stoichiometric benzaldehyde formation by bpy/$Cu^{II}(OTf)_2$/TEMPO under anaerobic conditions is significantly faster than the rate of aerobic catalytic turnover.

## Analysis of an Oxoammonium-Mediated Alcohol Oxidation Pathway

The involvement of oxoammonium species in alcohol oxidation is well established,[17] and Semmelhack proposed such an intermediate in his Cu/ TEMPO-catalyzed aerobic alcohol oxidation method (Scheme 1).[8] Moreover, oxoammonium intermediates have been detected directly with some Cu/TEMPO catalyst systems.[20] Several observations, however, demonstrate that an oxoammonium mechanism is not involved with the present catalyst system.

The mechanism in Scheme 1 implies that $Cu^{II}$ should be able to oxidize TEMPO to $TEMPO^{+}$. This possibility was probed by EPR spectroscopy. TEMPO was added to an acetonitrile solution of $Cu(OTf)_2$, bpy and NMI, at catalytic concentrations (10, 10, and 20 mM, respectively). The presence of TEMPO has little effect on the EPR parameters of the $Cu^{II}$ signal (Supporting Information Figure S3), and double integration of the spectra reveals a signal intensity consistent with the total concentration of [$Cu^{II}$] and [TEMPO] added to the solution.[21] The lack of reactivity between $Cu^{II}$ and TEMPO is further supported by cyclic voltammetry (CV). A cyclic voltammogram obtained from an acetonitrile solution of $Cu^{I}(OTf)$, bpy, NMI and TEMPO revealed the presence of a reversible $TEMPO^{+}$/ TEMPO wave at 0.24 V and a broad quasireversible signal corresponding to $Cu^{II}/Cu^{I}$ at $E_{1/2}$ ~ −0.32 V (vs $Fc^{+}$/Fc) (Figure 3; for additional CV data, see Supporting Information Figure S4).[22] The $TEMPO^{+}$/TEMPO redox feature is nearly identical to that observed with a solution containing TEMPO in the absence of the other reaction components. The presence of bpy dramatically lowers the $Cu^{II}/Cu^{I}$ reduction potential in acetonitrile, from +0.66 to −0.18 V, and this potential is lowered further in the presence of NMI (to −0.32 V). Collectively, these EPR and CV data show that $Cu^{II}$ is not capable of oxidizing TEMPO to $TEMPO^{+}$ under the present reaction conditions.

Kinetic evidence that $TEMPO^{+}$ is not the active oxidant under catalytic conditions was obtained by comparing the rates of oxidation of $PhCH_2OH$ and $CyCH_2OH$ by 1 equiv of the oxoammonium salt, $TEMPO^{+}OTf^{-}$, and by catalytic (bpy)$Cu^{I}$/ TEMPO (eq 1). These reactions were monitored by in situ IR spectroscopy, and the $TEMPO^{+}$-mediated alcohol oxidations were found to proceed more slowly than the catalytic reactions, despite the 20-fold higher concentration of oxoammonium present in the stoichiometric reaction (Figure 4). Thus, the oxoammonium cation is not kinetically competent to serve as the oxidant under catalytic conditions.

The lack of involvement of an oxoammonium species suggests that $Cu^{II}$ and TEMPO act in concert as one-electron oxidants to achieve the net two-electron alcohol-to-aldehyde

oxidation reaction. A simplified mechanism reffecting the overall reaction stoichiometry is depicted in Scheme 2.[23]

This mechanism features two separate half-reactions: (1) oxidation of the reduced catalyst, consisting of $Cu^{I}$ and TEMPOH, by $O_2$ and (2) alcohol oxidation mediated by $Cu^{II}$ and TEMPO. Building on the framework of this general mechanism, subsequent studies focused on elucidating fundamental steps associated with the two half-reactions and probing the origin of the reactivity differences between benzylic and aliphatic alcohols.[24]

## In Situ Spectroscopic Studies of Catalytic Reactions

UV–visible and EPR spectroscopic studies were performed to gain insight into the nature of the catalyst species present during the reaction. The reactions were performed in a 3-neck flask equipped with a UV–visible dip probe, an $O_2$ inlet, and a septum for removing aliquots for GC and EPR spectroscopic analyses. Aliquots removed for EPR analysis were immediately frozen at 77 K to stop further reaction. Representative spectral time courses obtained during the oxidation of $CyCH_2OH$ are shown Figure 5 (see Supporting Information Figure S5 for analogous data with $PhCH_2OH$). The optical absorption of the $Cu^{I}$ species was monitored at 550 nm (cf. Figure 5),[25] and simulation and double-integration of EPR spectra enabled quantitation of the $Cu^{II}$ and TEMPO radical concentrations. Reaction time-course plots, showing the concentrations of aldehyde, $Cu^{I}$, $Cu^{II}$ and TEMPO determined by GC and UV–visible and EPR spectroscopies during the oxidations of $PhCH_2OH$ and $CyCH_2OH$ are shown in Figure 6.[26]

In the oxidation of $PhCH_2OH$, formation of benzaldehyde exhibits a linear time course (Figure 6A, top plot), similar to that observed by in situ IR spectroscopy (cf. Figure 2). The copper species present in solution is predominantly $Cu^{I}$ (UV–visible, EPR). Only a minor decrease in $Cu^{I}$ was observed during the first 34 min of the reaction, after which the $Cu^{I}$ concentration decreased rapidly, coinciding with complete conversion of benzyl alcohol (GC). EPR analysis of the finished reaction mixture showed a $Cu^{II}$ signal that corresponded to 70% of the total Cu (data not shown), while UV–visible data indicated that all the Cu existed as $Cu^{II}$. This disparity can be explained by the partial formation of EPR-silent $Cu^{II}$ species, such as a hydroxide-bridged dimer, which was isolated at the end of the reaction.[27] The concentration of TEMPO radical detected by EPR spectroscopy is low throughout the entire time course and ranges from 17 to 32% of the TEMPO added.

In the oxidation of $CyCH_2OH$, formation of CyCHO exhibits a nonlinear time course, and $Cu^{I}$ evolves gradually into $Cu^{II}$ throughout the reaction (UV–visible, EPR) (Figure 6B). Furthermore, the concentration of TEMPO radical is relatively high throughout the reaction, corresponding to ~70% of the TEMPO added.

These observations suggest that the catalyst resting state changes, depending on the identity of the alcohol substrate. With $PhCH_2OH$, the majority of the catalyst is present as $Cu^{I}$. With $CyCH_2OH$, both $Cu^{I}$ and $Cu^{II}$ are present during the reaction and the ratio changes as substrate oxidation proceeds. According to the simplified mechanism in Scheme 2, these observations imply that “catalyst oxidation” is turnover limiting with the more reactive benzyl alcohol substrates, while both “substrate oxidation” and “catalyst oxidation” appear to contribute to the turnover rate with the less reactive substrate, $CyCH_2OH$.

## Catalytic Rate Laws

Kinetic studies were carried out to establish the rate laws for the oxidations of $PhCH_2OH$ and $CyCH_2OH$. The rates were determined by monitoring the change in oxygen pressure within a sealed, temperature-controlled reaction vessel using a computer-interfaced gas-uptake apparatus. Both oxidation reactions are well-behaved (eq 1, Supporting Information

Figures S7–S14), and initial rates were obtained from the gas uptake traces at ≤5% conversion.

The rate of oxidation of $PhCH_2OH$ exhibits a first-order dependence on the oxygen pressure (Figure 7A). Variation of the (bpy)$Cu^{I}OTf$ loading reveals a mixed-order dependence, with a second-order dependence at low [Cu] and a first-order dependence at high [Cu] (Figure 7B). No dependence is observed on [TEMPO] or [$PhCH_2OH$] (Figures 7C and 7D). Control experiments show that the first-order dependence on $pO_2$ does not arise from mass-transfer effects. For example, the rate continues to increase with increasing catalyst concentrations (Supporting Information Figure S15), and the reaction rate is unaffected by changes in the stirring rate.

Analogous kinetic studies were carried out for the oxidation of $CyCH_2OH$ (Figure 7A–7D). In this reaction, the catalytic rate again exhibits a first-order dependence on the oxygen pressure and a mixed second-order/first-order dependence on [Cu]; however, it exhibits a saturation dependence on [$CyCH_2OH$]. The reaction also displays a [TEMPO] dependence that is first-order with a nonzero intercept.[28] The latter two observations differ from the observations with $PhCH_2OH$. Further analysis of these data is presented below.

## Kinetic Isotope Effects

Several different types of deuterium kinetic isotope effects were determined for the oxidations of $PhCH_2OH$ and $CyCH_2OH$, (Table 1), including independent rate measurements for the oxidation of $RCH_2OH$ and $RCD_2OH$, and intermolecular and intramolecular competition experiments. Each of these studies provides unique insights into the reaction mechanism.[29]

The oxidations of PhCHDOH and CyCHDOH reveal a large kinetic isotope effect for the C–H cleavage step, $k_H/k_D$ = 6.06 and 10.9, respectively. Measurement of the independent rates for the oxidations of $PhCH_2OH$ and $PhCD_2OH$ showed no significant isotope effect ($k_H/k_D$ = 1.05), whereas the oxidations of $CyCH_2OH$ and $CyCD_2OH$ showed a significant isotope effect ($k_H/k_D$ = 3.5) (Table 1 and Figure 8). These data show that C–H cleavage is not turnover limiting in the reaction of $PhCH_2OH$, but it contributes to the turnover rate in the case of $CyCH_2OH$.[31] Intermolecular competition KIEs measured for $PhCH_2OH$ and $CyCH_2OH$ revealed KIEs of ~2 in both cases. The origin of the latter observations will be discussed below.

## Hammett Studies

Hammett studies were conducted for various *para*-substituted benzyl alcohols via independent rate measurements and via competition experiments. Comparison of the independently measured rates of the different alcohols reveals a negligible electronic dependence (Figure 9A). In contrast, a significant electronic dependence was obtained from competition studies, in which an equimolar quantity of a *para*-substituted benzyl alcohol and unsubstituted $PhCH_2OH$ were oxidized by $Cu^{I}$/TEMPO in the same reaction vessel. The product distribution was measured by $^1H$ NMR spectroscopy at early reaction times (<20% conversion). The Hammett plot (Figure 9B) reveals preferential oxidation of electron-defficient alcohols ($\rho$ = +0.33). The mechanistic origin of the differences between these two Hammett studies will be discussed below.

## Proposed Catalytic Mechanism

The UV–visible and EPR spectroscopic data described above show that the catalytic resting state and turnover-limiting step differ for benzylic and aliphatic alcohols. The catalyst appears to be predominantly $Cu^{I}$ and TEMPOH in the oxidation of $PhCH_2OH$, and aerobic

oxidation of $Cu^{I}$/TEMPOH establishes the turnover rate (cf. Scheme 2). In the oxidation of $CyCH_2OH$, both $Cu^{I}$/ TEMPOH and $Cu^{II}$/TEMPO are present in significant quantities during catalytic turnover, and their relative concentrations evolve throughout the reaction. The collective kinetic and spectroscopic data provide the basis for the more detailed catalytic mechanism in Scheme 3.

## Catalyst Oxidation by $O_2$

Both alcohols exhibit a similar kinetic dependence on [Cu] and [$O_2$] (cf. Figure 7). The first-order dependence on [$O_2$] and mixed second-order/first-order dependence [Cu] resembles reactions of $O_2$ with biomimetic nitrogen-chelated $Cu^{I}$ complexes,[32,33] and the data are consistent with a mechanism in which $O_2$ reacts with $Cu^{I}$ to afford a $Cu^{II}$-superoxide species, followed by reaction with a second $Cu^{I}$ center to generate a peroxo-bridged binuclear $Cu^{II}$ species, $Cu_2O_2$ (Scheme 3, steps 1 and 2). The structure of the $Cu_2O_2$ intermediate is not known, but could be a □□□: □□ or □1,2-peroxo species, or even a bis-□ oxo-$Cu^{III}_2$ species.[32,34] The rate law corresponding to this two-step sequence accounts for the second-order dependence on [Cu] at low [Cu], and first-order dependence at high [Cu] (eq 3). A double reciprocal plot of this kinetic expression allows determination of the rate constant $k_1$ and the ratio $k_{-1}/k_2$ from the intercept and slope, respectively (eq 4, Figure 10).

$$\text{rate}=\frac{k_1 k_2 [\text{Cu}]_{\text{tot}}^2 [\text{O}_2]}{k_{-1}+k_2[\text{Cu}]_{\text{tot}}} \quad (3)$$

$$\frac{[\text{Cu}]_{\text{tot}}}{\text{rate}}=\frac{k_{-1}}{k_1 k_2 [\text{Cu}]_{\text{tot}}[\text{O}_2]}+\frac{1}{k_1[\text{O}_2]} \quad (4)$$

Analogous rate constants have been measured for a number of biomimetic copper complexes at low temperatures (e.g., –90°C).[32] The values of $k_1$ reported in the literature span 10 orders of magnitude and have been shown to be strongly dependent on the ancillary ligands and the solvent.[33b] The value of $k_1$ determined for the present catalyst system ($k_1$ = 4.2 $M^{-1}$ $s^{-1}$) is significantly lower than those reported in the literature, which are commonly ~$10^2$–$10^4$ $M^{-1}$ $s^{-1}$ at 183 K.[33] Further studies will be needed to understand the origin of this difference, but it is tentatively attributed to the use of acetonitrile as the solvent and bpy as the ancillary ligand, both of which are known to stabilize $Cu^{I}$ and thereby disfavor the reaction with $O_2$. The ratio of $k_{-1}/k_2$ determined here is 3.8 × $10^{-3}$ $M^{-1}$, which reflects a more favorable forward reaction to the dimeric $Cu_2O_2$ intermediate relative to precedents in the literature ($k_{-1}/k_2$ is typically >1). Again, further studies are needed, but this difference may reffect the smaller steric profile of bpy relative to ligands employed in previous studies.

Steps 3–5 are proposed be fast under the reaction conditions. While these steps are not directly observed, analogous reactions have considerable precedent in the literature. In step 3, the $Cu_2O_2$ species is proposed to oxidize TEMPOH to TEMPO via H-atom transfer, forming a $Cu^{II}$–OOH species and $Cu^{I}$ as byproducts. $Cu_2O_2$-mediated abstraction of a hydrogen atom from O–H bonds, including TEMPO–H, to afford oxyl radicals is known.[35–39] Control experiments show that oxidation of $Cu^{I}$ to $Cu^{II}$ by $O_2$ does not require TEMPOH; however, TEMPOH appears to be required to achieve a kinetically competent rate. At the start of the reaction, when no TEMPOH is available, we speculate that the alcohol substrate reacts with the $Cu_2O_2$ species to afford $Cu^{II}$–OOH and $Cu^{II}$–$OCH_2R$ species.

Subsequent reaction of the $Cu^{II}$–OOH intermediate with water (or the alcohol substrate) will release $H_2O_2$ and afford a $Cu^{II}$–OH (or $Cu^{II}$–$OCH_2R$) species (step 4).[40] As described above

(cf. eq 2), $H_2O_2$ undergoes rapid disproportionation under the catalytic conditions. $H_2O_2$ disproportionation by (bpy)Cu complexes has been reported previously,[41] and this reaction (step 5) can account for the observed 2:1 alcohol/$O_2$ stoichiometry.

## Alcohol Oxidation by $Cu^{II}$/TEMPO

Oxidation of the alcohol substrate by $Cu^{II}$ and TEMPO is proposed to proceed via preequilibrium formation of a $Cu^{II}$–alkoxide, followed by H-atom abstraction by TEMPO (steps 6 and 7).[42] The saturation kinetic dependence on [$RCH_2OH$] and first-order dependence on [TEMPO] in the oxidation of $CyCH_2OH$ (Figures 7C and 7D) provide evidence for this stepwise sequence. A rate law reffecting these steps is shown in eq 5.

$$\text{rate} = \frac{K_6 k_7 [\text{Cu}]_{\text{tot}} [\text{RCH}_2\text{OH}] [\text{TEMPO}]}{1 + K_6 [\text{RCH}_2\text{OH}]} \quad (5)$$

Formation of the aldehyde from the $Cu^{II}$–alkoxide intermediate in step 7 consists of a two-electron/one-proton process in which $Cu^{II}$ and TEMPO work in concert. Both PhCHDOH and CyCHDOH exhibit large primary isotope effects in this C–H cleavage step (cf. Table 1). The kinetic data are consistent with a bimolecular reaction between TEMPO and the $Cu^{II}$-alkoxide, which contrasts previous mechanistic proposals that invoke H-atom abstraction from a TEMPO–$Cu^{II}$ adduct.[43–46] While such an adduct cannot be rigorously excluded, no direct kinetic and spectroscopic evidence supports such an intermediate.[47,48]

The KIEs obtained from the intermolecular competition experiments (Table 1C) provide evidence for rapid exchange between hydroxide/alkoxide or different alkoxide ligands at $Cu^{II}$ (e.g., step 6, Scheme 3). Independent oxidations of $PhCH_2OH$ and $PhCD_2OH$ show no difference in rate because turnover-limiting oxidation of $Cu^{I}$/TEMPOH is independent of [$RCH_2OH$]. However, the 2-fold preference for oxidation of $PhCH_2OH$ over $PhCD_2OH$ in a competition experiment can arise from reversible formation of the $Cu^{II}$-alkoxides, which enables kinetic selection of $Cu^{II}$–$OCH_2R$ over $Cu^{II}$–$OCD_2R$.

The Hammett data obtained with substituted benzyl alcohols (Figure 9) provide complementary insights. No electronic dependence is detected when each of the alcohols is oxidized independently (Figure 9A), but preferential oxidation of the more-electron-defficient substrate is observed in a mixture of two benzyl alcohols (Figure 9B). This outcome can be rationalized by preferential formation of the $Cu^{II}$–$OCH_2R$ species derived from the more acidic alcohol.[49] If kinetic selectivity were controlled by the H-atom abstraction step, a negative Hammett slope would be expected. That a negative Hammett slope has been observed in the oxidation of benzylic alcohols by the CuCl/TEMPO catalyst system (i.e., without bpy; $\rho = -0.14$)[13a] suggests different catalyst systems can exhibit different selectivity patterns.

The mechanism in Scheme 3 provides a rationale for the historical challenge associated with the oxidation of aliphatic alcohols with Cu/TEMPO and related catalyst systems. Aliphatic alcohols have O–H bonds with p$K_a$ values ~2 units higher than those of benzylic alcohols,[49,50] a property that will significantly hinder formation of the Cu-alkoxide intermediate in step 6. Moreover, their C–H bonds are 8–10 kcal $mol^{-1}$ stronger than those of benzylic alcohols ($BDE_{aliphatic}$ ~ 93 kcal $mol^{-1}$; $BDE_{benzylic}$ ~ 83–85 kcal $mol^{-1}$).[51] The more challenging oxidation of aliphatic alcohols is manifested in the differences between the catalytic rate laws for the two substrates. With benzyl alcohol, the substrate oxidation steps are sufficiently facile that the rate is controlled exclusively by the reaction of $Cu^{I}$ with $O_2$. In the oxidation of $CyCH_2OH$, however, steps 6 and 7 contribute significantly to the turnover rate (cf. Figure 7). That the rate of the latter reaction retains a dependence on

$pO_2$ indicates that a delicate kinetic balance exists among the steps associated with substrate oxidation and reaction of the reduced catalyst with $O_2$.

Abstraction of a hydrogen atom from the $Cu^{II}$-alkoxide by TEMPO (step 7) is intriguing because the BDE of TEMPO–H is only ~71 kcal $mol^{-1}$,[51] which is considerably lower than the α-C–H BDE of the corresponding alcohols. Thus, the α-C–H bond must be significantly weakened upon formation of the $Cu^{II}$-alkoxide. Step 7 is not a simple H-atom transfer reaction (i.e., a 1 $H^+$/1 $e^-$ step), however, because it occurs with concomitant, and possibly concerted, reduction of $Cu^{II}$ to $Cu^{I}$. Thus, this reaction corresponds to 1 $H^+$/2 $e^-$ transfer step. To our knowledge, such steps have not been systematically investigated.[52]

Our previous report on the development of this catalyst system[6a] highlighted the high chemoselectivity for primary over secondary alcohols. This selectivity most likely reflects strong steric effects on the bimolecular reaction between TEMPO and the $Cu^{II}$-alkoxide; however, the slightly higher p$K_a$ of secondary alcohols [ Δp$K_a$(2°–1°) ~ 1[50]) also should contribute to the difference in reactivity.

## CONCLUSIONS

This study has provided extensive insights into the catalytic mechanism of (bpy)$Cu^{I}$/TEMPO-catalyzed aerobic oxidation of alcohols. The overall mechanism differs substantially from other TEMPO-catalyzed alcohol oxidation reactions that involve an oxoammonium ($TEMPO^+$) intermediate. Instead, the (bpy)$Cu^{I}$/TEMPO-catalyzed reactions more closely resemble galactose oxidase, in which $Cu^{II}$ and an oxyl radical operate jointly as one-electron oxidants to mediate the two-electron alcohol oxidation reaction. While a thorough comparison of (bpy)$Cu^{I}$/TEMPO and galactose oxidase is beyond the scope of this discussion,[13] the results of our study also reveal differences between the synthetic and enzymatic catalysts. For example, in galactose oxidase, a single Cu center reacts with $O_2$, whereas the (bpy)$Cu^{I}$/TEMPO catalyst system involves the reaction of two Cu centers with $O_2$, thereby more closely resembling the $O_2$ activation by binuclear type 3 Cu enzymes, such as tyrosinase.[32] Moreover, galactose oxidase and related biomimetic catalysts[14–16] afford $H_2O_2$ as a byproduct, while (bpy)$Cu^{I}$/TEMPO consumes all four oxidizing equivalents from $O_2$, yielding $H_2O$ as a byproduct. These similarities and differences between synthetic and enzymatic catalysts and their implications for the development of new aerobic oxidation reactions are worthy of future investigation.

This study also provides clear insights into the factors that differentiate the reactivity of benzylic and aliphatic alcohols. Specifically, the reactivity of aliphatic alcohols is hindered relative to benzylic alcohols by the higher p$K_a$ of the hydroxyl group and the stronger α-C–H bond. These factors contribute to a change in the identity of the catalyst resting state and turnover-limiting step in the catalytic reaction: a $Cu^{I}$ resting state prevails in the oxidation of the benzylic alcohol, while a mixed $Cu^{I}$/$Cu^{II}$ resting state is present during the oxidation of the less reactive aliphatic alcohol. Similarly, the rate of alcohol oxidation is controlled exclusively by aerobic oxidation of $Cu^{I}$ in the case of the benzylic alcohol, while multiple steps are kinetically relevant with the aliphatic alcohol. These observations suggest that the optimal catalyst will differ for different classes of alcohols, and efforts to exploit these insights in the development of improved catalysts have been initiated.

## EXPERIMENTAL SECTION

### Instrumentation

$^1H$ and $^{13}C\{^1H\}$ NMR spectra were recorded on a Bruker Avance 300 MHz spectrometer. Chemical shifts ( δ) are given in parts per million and referenced to the residual solvent

signal.[53] In situ IR kinetics were performed using a Mettler Toledo ReactIR ic10 with an AgX probe. EPR spectra were recorded on a Bruker EleXsys E500 spectrometer at 150 K under nonsaturating conditions. Spin quantitation was performed by baseline-corrected double integration of spectra relative to calibration curves. UV–visible spectra were acquired using a Blue-Wave spectrometer system with a fiber optic dip probe from StellarNet. Spectral deconvolution for time courses was performed via Singular Value Decomposition/Evolving Factor Analysis (SVD/EFA) was performed using ReactLab software (Jplus Consulting). Gas chromatographic analyses were performed on a Shimadzu GC-2010 Plus gas chromatograph with a Restek RTX-5 (15 m) column with trimethoxybenzene as an internal standard. Electrochemical measurements were conducted on a BASi Epsilon EC potentiostat using a platinum-button working electrode, nonaqueous $Ag/Ag^+$ reference and a platinum wire counter electrode at a scan rate of 100 mV/s, unless otherwise noted. Elemental analyses were performed by Atlantic Microlab, Norcross, GA. Melting points were taken on a Mel-Temp II melting point apparatus. Column chromatography was performed on an Isco Combiflash system using Silicycle 60 silica gel.

## Reagents

All commercial reagents were obtained from Aldrich and used as received unless otherwise noted. $CH_3CN$ was obtained from solvent purification columns, in which the solvent is passed through a column of activated molecular sieves.

## Gas Uptake Kinetics

Each set of data was collected using a 6-well gas uptake apparatus that holds six volume-calibrated 50 mL round-bottom flasks, independently connected to a pressure transducer designed to measure the gas pressure within each sealed reaction vessel.[3a] Five vessels were use for the reaction mixtures, and the sixth well used as a solvent control to account for variations in pressure. The apparatus was evacuated and filled with $O_2$ to 800 Torr three times. The pressure was then established at 500 Torr and the flasks heated to 27 °C. A solution of alcohol was added via syringe through a septum, and the pressure and temperature allowed to equilibrate. When the pressure (approximately 600 Torr) and temperature (27 °C) stabilized, a solution of catalyst was added via syringe through a septum. Details for the alcohol and catalyst solutions used in each experiment are described in the Supporting Information.

Data were acquired using custom software written within LabVIEW (National Instruments). The data in Figure 7 was obtained from linear fits to early reaction times of the time course traces. Error bars shown are 2× the standard deviation of the rate acquired from three independent experiments.

## ReactIR Kinetics

A typical reaction was conducted as follows. A three-neck flask containing the alcohol (0.5 mmol) in MeCN (2.0 mL) and a stir bar was secured in a temperature controlled bath at 27 °C. Two necks were fitted with septa, one holding an $O_2$ balloon attached to a syringe. The third neck was used for the IR dip probe (Mettler Toledo ReactIR ic10 with an AgX probe). A full spectrum was collected every 15 s. The reaction was initiated (after data collection began) by addition of a solution of catalyst. The absorbance at a particular frequency was plotted as a function of time.

## EPR and UV–Visible Time Course Data

A typical reaction was conducted as follows. A 100 mL three-neck flask under one atmosphere of $O_2$ at room temperature, containing $[Cu^I(MeCN)_4]$-(OTf) (0.30 mmol), bpy

(0.30 mmol), TEMPO (0.30 mmol), and NMI (0.60 mmol) in acetonitrile was fitted with two septa and a UV–visible dip probe spectrometer. Alcohol (6 mmol) was injected and the reaction was monitored in situ by UV–visible spectroscopy. 0.5 mL aliquots were removed and flash frozen in liquid nitrogen for EPR analysis, and 0.1 mL aliquots were removed, diluted with EtOAc and filtered through a silica plug for GC analysis.

### Electrochemistry

In a 0.3 M $LiClO_4$ buffer, cyclic voltammograms of $Cu^{I}(OTf)(MeCN)_4$ in the presence of catalytic components were acquired under $N_2$ in acetonitrile with a platinum working electrode. In all cases, the $Cu^{I}/Cu^{II}$ couples were not fully reversible on the CV time scale at scan rates from 10 to 500 mV/s.

## Supplementary Material

Refer to Web version on PubMed Central for supplementary material.

## Acknowledgments

We thank Professor Clark Landis for mechanistic discussion and insight. We are grateful to the DOE (DE-FG02-05ER15690), the ACS GCI Pharmaceutical Roundtable, the Camille and Henry Dreyfus Postdoctoral Program in Environmental Chemistry for research grants, and NIH for a training grant (CBIT NIGMS T32 GM008505) that supported B.L.R. NMR spectroscopy facilities were partially supported by the NSF (CHE-9208463) and NIH (S10 RR08389), and the EPR facility was partially supported by the NSF (CHE-9629688).

## References

1. (a) Tojo, G.; Fernández, M. Oxidation of Alcohols to Aldehydes and Ketones. Tojo, G., editor. Springer; New York: 2010. (b) Tojo, G.; Fernández, M. Oxidation of Primary Alcohols to Carboxylic Acids. Tojo, G., editor. Springer; New York: 2010.
2. For representative recent reviews, see: Arends IWCE, Sheldon RA. Bäckvall J-E. In Modern Oxidation Methods. Wiley-VCH Verlag Gmb & CoWeinheim2004:83–118.Sheldon RA, Arends IWCE, ten Brink G-J, Dijksman A. Acc Chem Res. 2002; 35:774–781. [PubMed: 12234207] Zhan BZ, Thompson A. Tetrahedron. 2004; 60:2917–2935.Mallat T, Baiker A. Chem Rev. 2004; 104:3037–3058. [PubMed: 15186187] Stahl SS. Angew Chem, Int Ed. 2004; 43:3400–3420.Markó IE, Giles PR, Tsukazaki M, Chellé-Regnaut I, Gautier A, Dumeunier R, Philippart F, Doda K, Mutonkole JL, Brown SM, Urch CJ. Adv Inorg Chem. 2004; 56:211–240.Schultz MJ, Sigman MS. Tetrahedron. 2006; 62:8227–8241.Sigman MS, Jensen DR. Acc Chem Res. 2006; 39:221–229. [PubMed: 16548511] Matsumoto T, Ueno M, Wang N, Kobayashi S. Chem-Asian J. 2008; 3:196–214. [PubMed: 18232022] Karimi B, Zamani A. J Iran Chem Soc. 2008; 5:S1–S20.Parmeggiani C, Cardona F. Green Chem. 2012; 14:547–564.
3. For representative studies from our lab, see: Steinhoff BA, Guzei IA, Stahl SS. J Am Chem Soc. 2004; 126:11268–11278. [PubMed: 15355108] Steinhoff BA, Stahl SS. J Am Chem Soc. 2006; 128:4348–4355. [PubMed: 16569011]
4. For reviews describing homogeneous Pd catalysts for aerobic alcohol oxidation, see refs 2b, 2c, 2e, 2g, 2h, 2j, and 2k.
5. Ye X, Johnson MD, Diao T, Yates MH, Stahl SS. Green Chem. 2010; 12:1180–1186. [PubMed: 20694169]
6. (a) Hoover JM, Stahl SS. J Am Chem Soc. 2011; 133:16901–16910. [PubMed: 21861488] (b) Hoover JM, Steves JE, Stahl SS. Nat Protoc. 2012; 7:1161–1166. [PubMed: 22635108]
7. (a) Brackman W, Gaasbeek C. Recl Trav Chim. 1966; 85:221–241.(b) Brackman W, Gaasbeek C. Recl Trav Chim. 1966; 85:257–267.
8. Semmelhack MF, Schmid CR, Cortés DA, Chou CS. J Am Chem Soc. 1984; 106:3374–3376.
9. (a) Tretyakov VP, Chudaev VV, Zimtseva GP. Ukr Khim Zh. 1985; 51:942–946.(b) Betzemeier B, Cavazzini M, Quici S, Knochel P. Tetrahedron Lett. 2000; 41:4343–4346.(c) Ragagnin G,

Betzemeier B, Quici S, Knochel P. Tetrahedron. 2002; 58:3985–3991.(d) Gamez P, Arends IWCE, Reedijk J, Sheldon RA. Chem Commun. 2003:2414–2415.(e) Gamez P, Arends IWCE, Sheldon RA, Reedijk J. Adv Synth Catal. 2004; 346:805–811.(f) Geisslmeir D, Jary WG, Falk H. Monatsh Chem. 2005; 136:1591–1599.(g) Jiang N, Ragauskas AJ. J Org Chem. 2006; 71:7087–7090. [PubMed: 16930071] (h) Velusamy S, Srinivasan A, Punniyamurthy T. Tetrahedron Lett. 2006; 47:923–926.(i) Chung CWY, Toy PH. J Comb Chem. 2007; 9:115–120. [PubMed: 17206839] (j) Figiel PJ, Leskelä M, Repo T. Adv Synth Catal. 2007; 349:1173–1179.(k) Lu Z, Costa JS, Roubeau O, Mutikainen I, Turpeinen U, Teat SJ, Gamez P, Reedijk J. Dalton Trans. 2008:3567–3573. [PubMed: 18594705] (l) Jiang N, Ragauskas AJ. ChemSusChem. 2008; 1:823–825. [PubMed: 18798206] (m) Kumpulainen ETT, Koskinen AMP. Chem—Eur J. 2009; 15:10901–10911. [PubMed: 19746477] (n) Figiel PJ, Sibaouih A, Ahmad JU, Nieger M, Räisänen MT, Leskelä M, Repo T. Adv Synth Catal. 2009; 351:2625–2632.(o) Hu Z, Kerton FM. Appl Catal, A. 2012; 413:332–339.(p) Könning D, Hiller W, Christmann M. Org Lett. 2012; 14:5258–5261. [PubMed: 23039225]

10. For additional examples of Cu/TEMPO that do not use a chelating nitrogen ligand, see: Ansari IA, Gree R. Org Lett. 2002; 4:1507–1509. [PubMed: 11975615] Jiang N, Ragauskas AJ. Org Lett. 2005; 7:3689–3692. [PubMed: 16092851] Mannam S, Alamsetti SK, Sekar G. Adv Synth Catal. 2007; 349:2253–2258.Tromp SA, Matijošytė I, Sheldon RA, Arends IWCE, Mul G, Kreutzer MT, Moulijn JA, de Vries S. ChemCatChem. 2010; 2:827–833.
11. (a) Sonobe T, Oisaki K, Kanai M. Chem Sci. 2012; 3:3249–3255.(b) Han B, Yang XL, Wang C, Bai YW, Pan TC, Chen X, Yu W. J Org Chem. 2012; 77:1136–1142. [PubMed: 22168403] (c) Hu Z, Kerton FM. Org Biomol Chem. 2012; 10:1618–1624. [PubMed: 22231227] (d) Flanagan JCA, Dornan LM, McLaughlin MG, McCreanor NG, Cook MJ, Muldoon MJ. Green Chem. 2012; 14:1281–1283.(e) Tian H, Yu X, Li Q, Wang J, Xu Q. Adv Synth Catal. 2012; 354:2671–2677.
12. For mechanistic studies of other Cu/TEMPO-catalyzed oxidation reactions, see refs 9m and 13a.
13. For example, see: Dijksman A, Arends IWCE, Sheldon RA. Org Biomol Chem. 2003; 1:3232–3237. [PubMed: 14527157] Sheldon RA, Arends IWCE. J Mol Catal A: Chem. 2006; 251:200–214.Que L, Tolman WB. Nature. 2008; 455:333–340. [PubMed: 18800132]
14. Whittaker JW. Chem Rev. 2003; 103:2347–2363. [PubMed: 12797833]
15. For a review of biomimetic Cu/phenoxyl-radical complexes that mediate aerobic oxidation of alcohols see: Thomas F. Eur J Inorg Chem. 2007; 2007:2379–2404.
16. See also the following leading references: Wang Y, DuBois JL, Hedman B, Hodgson KO, Stack TDP. Science. 1998; 279:537–540. [PubMed: 9438841] Chaudhuri P, Hess M, Flörke U, Wieghardt K. Angew Chem, Int Ed. 1998; 37:2217–2220.Chaudhuri P, Hess M, Meyhermüller T, Wieghardt K. Angew Chem, Int Ed. 1999; 38:1095–1098.Chaudhuri P, Hess M, Müller J, Hildenbrand K, Bill E, Weyhermüller T, Wieghardt K. J Am Chem Soc. 1999; 121:9599–9610.
17. For an overview see ref 1a. Additionally, see: Semmelhack MF, Chou CS, Cortes DA. J Am Chem Soc. 1983; 105:4492–4494.Anelli PL, Biffi C, Montanari F, Quici S. J Org Chem. 1987; 52:2559–2562.For a mechanistic rationale of selectivity patterns with oxoammonium-mediated oxidations see: Bailey WF, Bobbitt JM, Wiberg KB. J Org Chem. 2007; 72:4504–4509. [PubMed: 17488040]
18. For leading references, see: Golubev VA, Rozantsev EG, Neiman MB. Bull Acad Sci USSR. 1965:1898–1904.Miyazawa T, Endo T, Shiihashi S, Okawara M. J Org Chem. 1985; 50:1332–1334.Bobbitt JM. J Org Chem. 1998; 63:9367–9374.Qiu JC, Pradhan PP, Blanck NB, Bobbitt JM, Bailey WF. Org Lett. 2011; 14:350–353. [PubMed: 22149048]
19. During catalytic reactions, a strong base is supplied in the form of hydroxide from the reduction of $O_2$. The requirement of suitably strong base complicates direct comparison of the stoichiometric reaction with catalytic reactions. Systematic investigation of base effects and the relative reactivity of $Cu^{I}$ vs $Cu^{II}$ catalyst precursors are the subject of ongoing investigation.
20. See ref 10d. and the following: Cecchetto A, Fontana F, Minisci F, Recupero F. Tetrahedron Lett. 2001; 42:6651–6653.
21. Sheldon and co-workers proposed that TEMPO oxidizes $Cu^{I}$ to $Cu^{II}$ in their study of the CuCl/TEMPO catalyst system, which lacks bpy as an ancillary ligand (ref 13a). A control experiment indicates that this reaction does not occur with the present catalyst system. The catalyst components ($Cu^{I}$OTf, bpy, NMI and TEMPO) were combined in acetonitrile under anaerobic conditions. EPR analysis of this mixture revealed no loss of TEMPO and no formation of $Cu^{II}$.

22. CV conditions: 2.5 mM Cu(OTf), 2.5 mM bpy, 5 mM NMI, 2.5 mM TEMPO, MeCN, under $N_2$. Referenced to $Cp_2Fe^{III}/Cp_2Fe^{II}$ external reference, scan rate = 100 $mV{\cdot}s^{-1}$, Pt button working electrode, 0.5 M $LiClO_4$ electrolyte.
23. For related mechanisms proposed with other Cu/TEMPO catalyst systems, see refs 9a, d, 10c, 11a, and 13a, and the following: Hill NJ, Hoover JM, Stahl SS. J Chem Educ. 2013; 90:102–105.
24. Although TEMPOH oxidation in the absence of Cu does occur, this reaction is considerably slower than catalytic turnover. Metal-free aerobic regeneration of TEMPO has been proposed previously in Cu/ TEMPO alcohol oxidation systems (e.g., see ref 13a).
25. A UV–visible spectrum of the catalytically relevant $Cu^I$ species was determined from a solution containing $(bpy)Cu^I(OTf)$, NMI, TEMPO, and $PhCH_2OH$ under $N_2$.
26. Deconvolution of the full UV–visible spectra with spectral fitting software, rather than single-wavelength data, yielded analogous $Cu^I$ and $Cu^{II}$ speciation time course data (Figure S6).
27. Control experiments indicate $[(bpy)Cu^{II}(\mu\text{-}OH)]_2$ can be used as a catalyst precursor for the oxidation of $PhCH_2OH$ and $CyCH_2OH$; however, the catalytic rates are somewhat slower than those observed under standard conditions. For previous characterization of this species, see: Garribba E, Micera G, Sanna D, Strinna-Erre L. Inorg Chim Acta. 2000; 299:253–261.
28. The nonzero intercept implicates a two-term rate law, one first-order in [TEMPO] and the other zero-order in [TEMPO]. The mechanistic basis for the zero-order term is not yet understood. Negligible alcohol oxidation occurs in the absence of TEMPO.
29. Simmons EM, Hartwig JF. Angew Chem, Int Ed. 2012; 51:3066–3072.
30. Semmelhack MF, Schmid CR, Cortes DA. Tetrahedron Lett. 1986; 27:1119–1122.
31. The KIEs determined from independent rate measurements of $RCH_2OH$ and $RCD_2OH$ do not vary at different alcohol concentrations (Figure S17).
32. For reviews, see: Lewis EA, Tolman WB. Chem Rev. 2004; 104:1047–1076. [PubMed: 14871149] Mirica LM, Ottenwaelder X, Stack TDP. Chem Rev. 2004; 104:1013–1045. [PubMed: 14871148] Hatcher LQ, Karlin KD. Adv Inorg Chem. 2006; 58:131–184.
33. For representative kinetic studies, see: Lee Y, Park GY, Lucas HR, Vajda PL, Kamaraj K, Vance MA, Milligan AE, Woertink JS, Siegler MA, Narducci Sarjeant AA, Zakharov LN, Rheingold AL, Solomon EI, Karlin KD. Inorg Chem. 2009; 48:11297–11309. [PubMed: 19886646] Zhang CX, Kaderli S, Costas M, Kim E-i, Neuhold Y-M, Karlin KD, Zuberbühler AD. Inorg Chem. 2003; 42:1807–1824. [PubMed: 12639113] Kobayashi Y, Okubo K, Nomura T, Kubo M, Fujieda N, Sugimoto H, Fukuzumi S, Goto K, Ogura T, Itoh S. Eur J Inorg Chem. 2012; 2012:4574–4578.
34. Preliminary efforts to directly observe Cu-superoxo or Cu-peroxo intermediates by UV–visible spectroscopy have not been successful, but further work in this area is ongoing.
35. A side-on $Cu^{II}_2(\mu\text{-}\eta^2\text{:-}\eta^2\text{-peroxo})$ complex in equilibrium with a $Cu^{III}_2(\mu\text{-oxo})_2$ complex reacts with TEMPO–H to afford TEMPO and unidentified Cu products (ref 32c).
36. An end-on $Cu^{II}_2(\mu\text{-}1,2\text{-peroxo})$ complex reacts with weak C–H bonds via H-atom abstraction to afford a $Cu^{II}OOH$ complex: Comba P, Haaf C, Helmle S, Karlin KD, Pandian S, Waleska A. Inorg Chem. 2012; 51:2841–2851. [PubMed: 22332786]
37. $Cu^{II}$-superoxo complexes have been shown to react with TEMPO–H to generate $Cu^{II}OOH$ complexes: Maiti D, Lee D-H, Gautchenova K, Würtele C, Holthausen MC, Narducci Sarjeant AA, Sundermeyer J, Schindler S, Karlin KD. Angew Chem, Int Ed. 2008; 47:82–85.
38. Karlin et al. reported a comparison of the reactivity of a series of end-on and side-on $Cu^{II}_2(\mu\text{-peroxo})$ structures with phenols. The two end-on $Cu^{II}_2(\mu\text{-}1,2\text{-peroxo})$ complexes deprotonate the phenol to afford Cu-hydroperoxo complexes, whereas the side-on $Cu^{II}_2(\mu\text{-}\eta^2\text{:-}\eta^2\text{-peroxo})$ complex promotes radical-mediated phenol coupling, with the formation of ill-defined Cu products: Paul PP, Tyeklar Z, Jacobson RR, Karlin KD. J Am Chem Soc. 1991; 113:5322–5332.
39. Stack et al. recently reported a $Cu^{II}_2(\mu\text{-}\eta^2\text{:-}\eta^2\text{-peroxo})$ species that does not react with TEMPO–H. This observation, together with those in refs 35–38, suggests that the identity of the reactive $Cu_2O_2$ intermediate cannot be inferred from its reactivity with TEMPOH. See: Citek C, Lyons CT, Wasinger EC, Stack TDP. Nat Chem. 2012; 4:317–322. [PubMed: 22437718]
40. The reversible protonolysis of a $Cu^{II}$-hydroperoxo has recently been demonstrated: Kim S, Saracini C, Siegler MA, Drichko N, Karlin KD. Inorg Chem. 2012; 51:12603–12605. [PubMed: 23153187]

41. (a) Sigel H, Flierl C, Griesser R. J Am Chem Soc. 1969; 91:1061–1064.(b) Sigel H, Wyss K, Fischer BE, Prijs B. Inorg Chem. 1979; 18:1354–1358.
42. Attempts to synthesize a well-defined (bpy)Cu–alkoxide species suitable for systematic investigation have, thus far, been unsuccessful.
43. Cu/TEMPO adducts: Caneschi A, Grand A, Laugier J, Rey P, Subra R. J Am Chem Soc. 1988; 110:2307–2309.Laugier J, Latour JM, Caneschi A, Rey P. Inorg Chem. 1991; 30:4474–4477.
44. A well-defined $Fe^{III}$-TEMPO adduct was recently shown to react with a secondary benzylic alcohol: Scepaniak JJ, Wright AM, Lewis RA, Wu G, Hayton TW. J Am Chem Soc. 2012; 134:19350–19353. [PubMed: 23134421]
45. Cu-TEMPO adducts relevant to alcohol oxidation have been studied computationally: Belanzoni P, Michel C, Baerends EJ. Inorg Chem. 2011; 50:11896–11904. [PubMed: 22050120] Cheng L, Wang J, Wang M, Wu Z. Inorg Chem. 2010; 49:9392–9399. [PubMed: 20849129] Michel C, Belanzoni P, Gamez P, Reedijk J, Baerends EJ. Inorg Chem. 2009; 48:11909–11920. [PubMed: 19938864]
46. Additional transition-metal complexes of nitroxyl radicals are known in the literature. For several examples not involving copper, see ref 44 and Dickman MH, Doedens RJ. Inorg Chem. 1982; 21:682–684.Mahanthappa MK, Huang KW, Cole AP, Waymouth RM. Chem Commun. 2002:502–503.Isrow D, Captain B. Inorg Chem. 2011; 50:5864–5866. [PubMed: 21591738] Smith JM, Mayberry DE, Margarit CG, Sutter J, Wang H, Meyer K, Bontchev RP. J Am Chem Soc. 2012; 134:6516–6519. [PubMed: 22452612]
47. For additional data, see Figure S3 and Table S1 in the Supporting Information.
48. A similar proposal has recently been made on the basis of EPR data for a catalyst employing a tetrapyridyl ligand: Gamba I, Mutikainen I, Bouwman E, Reedijk J, Bonnet S. Eur J Inorg Chem. 2013:115–123.
49. For $pK_a$ values of benzyl alcohols, see: Bordwell FG, Liu WZ. J Am Chem Soc. 1996; 118:8777–8781.
50. Olmstead WN, Margolin Z, Bordwell FG. J Org Chem. 1980; 45:3295–3299.
51. Luo, Y-R. Handbook of Bond Dissociation Energies in Organic Compounds. CRC-Press; Boca-Raton, FL: 2003.
52. We appreciate valuable discussions with Prof. James Mayer (University of Washington—Seattle) concerning this point.
53. Gottlieb HE, Kotlyar V, Abraham N. J Org Chem. 1997; 62:7512–7515. [PubMed: 11671879]

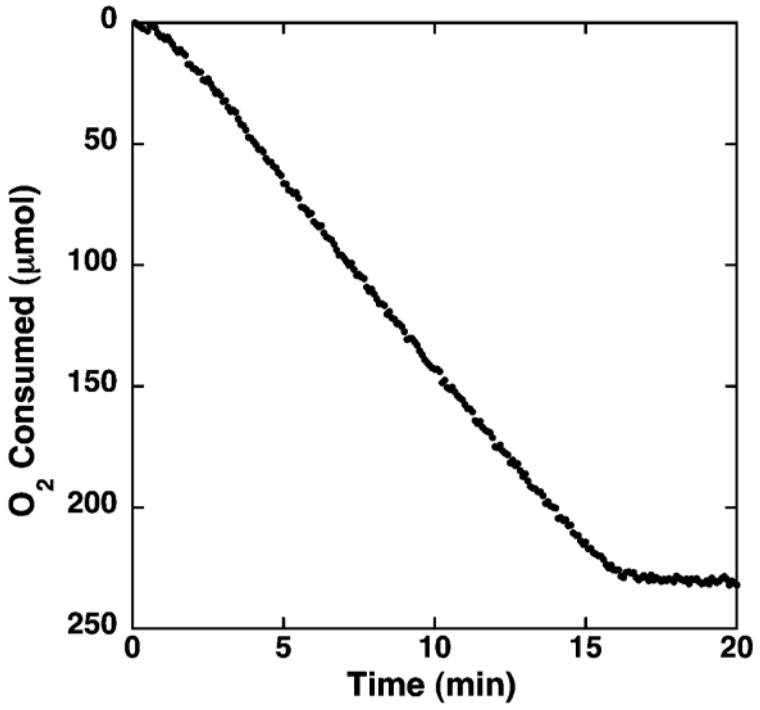


**Figure 1.**

Consumption of $O_2$ in the oxidation of $PhCH_2OH$ by (bpy)$Cu^I$/TEMPO monitored by gas uptake methods. Conditions: 200 mM $PhCH_2OH$ (500 $\mu$mol), 10 mM $Cu^I$(OTf), 10 mM bpy, 20 mM NMI, 10 mM TEMPO, initial $pO_2$ = 600 Torr, 2.5 mL MeCN, 27 °C.

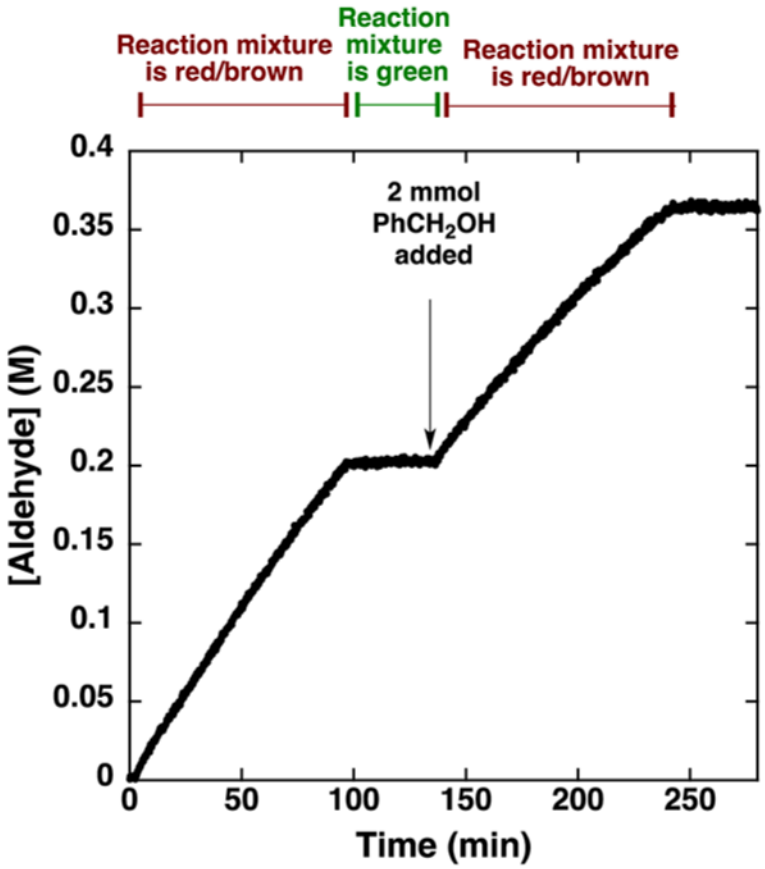


**Figure 2.**

Formation of benzaldehyde in the oxidation of $PhCH_2OH$ by (bpy)$Cu^I$/TEMPO monitored by in situ IR spectroscopy. Conditions: 10 mM $Cu^I$(OTf), 10 mM bpy, 20 mM, NMI, 10 mM TEMPO, 27 °C, 2 mL MeCN, air balloon, 2 mmol $PhCH_2OH$ in each addition.

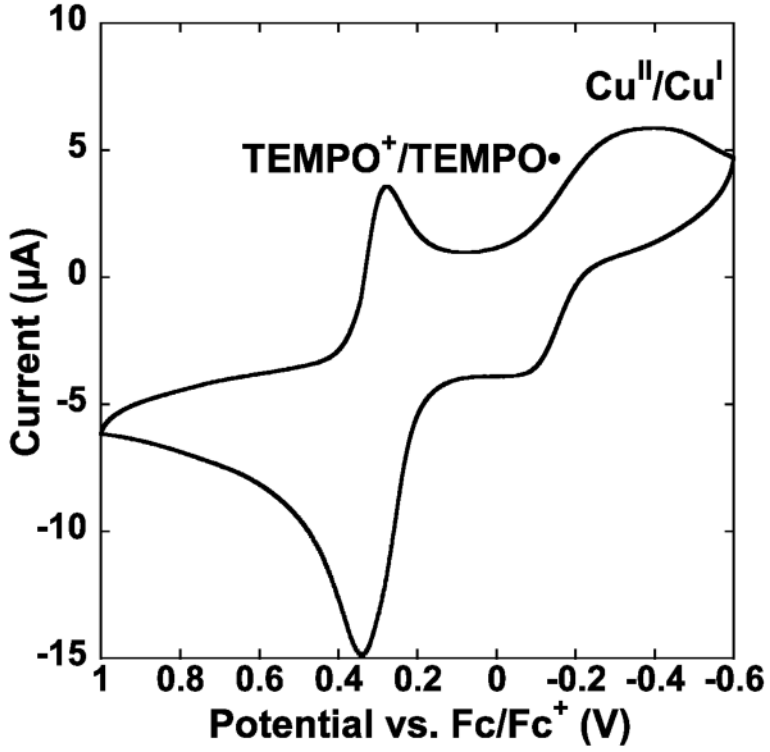


**Figure 3.**

Cyclic voltammogram of fully constituted catalyst mixture. Conditions: 2.5 mM $Cu^{I}$(OTf), 2.5 mM bpy, 2.5 mM TEMPO, 5 mM NMI, 500 mM $LiClO_4$, under $N_2$, 100 mV/s scan rate.

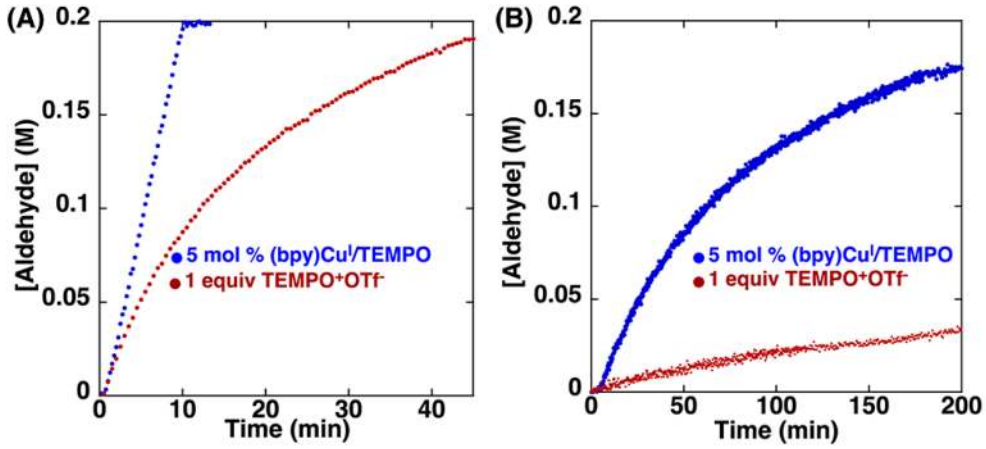


**Figure 4.**

Formation of aldehyde in the oxidation of (A) $PhCH_2OH$ and (B) $CyCH_2OH$ by 5 mol % (bpy)$Cu^{I}$/TEMPO (blue) and $TEMPO^{+}OTf^{-}$ (red) monitored by IR spectroscopy.

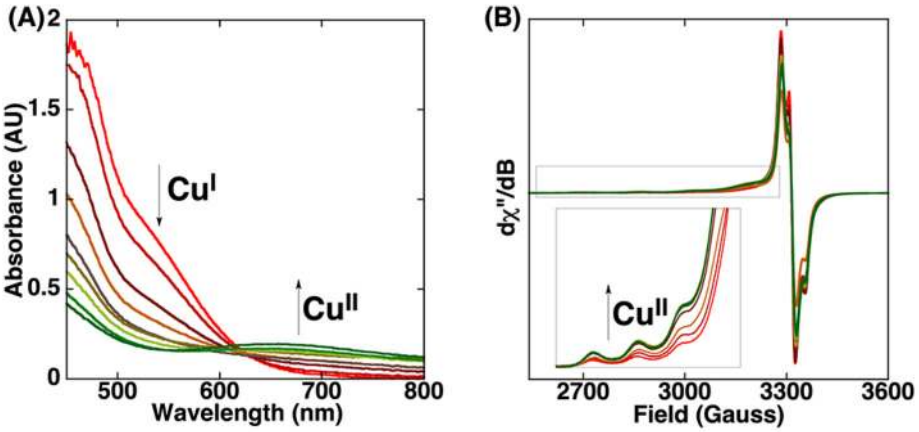


**Figure 5.**

(A) UV–visible and (B) EPR spectra acquired from monitoring the reaction time course for the oxidation of $CyCH_2OH$ by $(bpy)Cu^{I}(OTf)$/TEMPO. For analogous experiments with $PhCH_2OH$, see Figure S5.

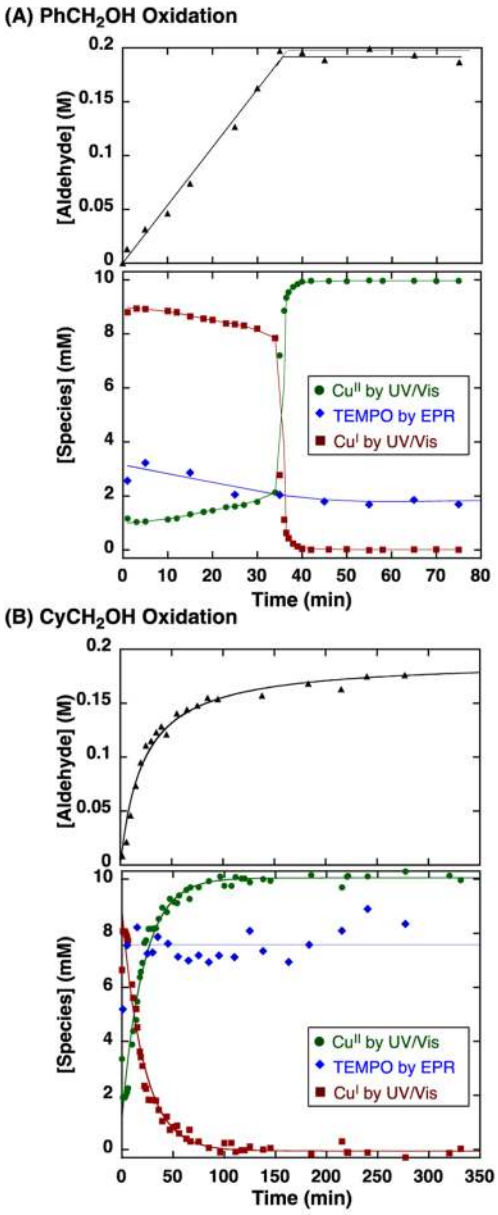


**Figure 6.**

Time-course data for the oxidation of (A) $PhCH_2OH$ and (B) $CyCH_2OH$ by (bpy)$Cu^I(OTf)$/TEMPO. Conditions: 0.2 M $RCH_2OH$, 10 mM $Cu^I(MeCN)_4OTf$, 10 mM bpy, 20 mM NMI, 10 mM TEMPO, 25 mL MeCN, 1 atm $O_2$, rt. The lines are included simply as visual aids and do not reffect kinetic fits.

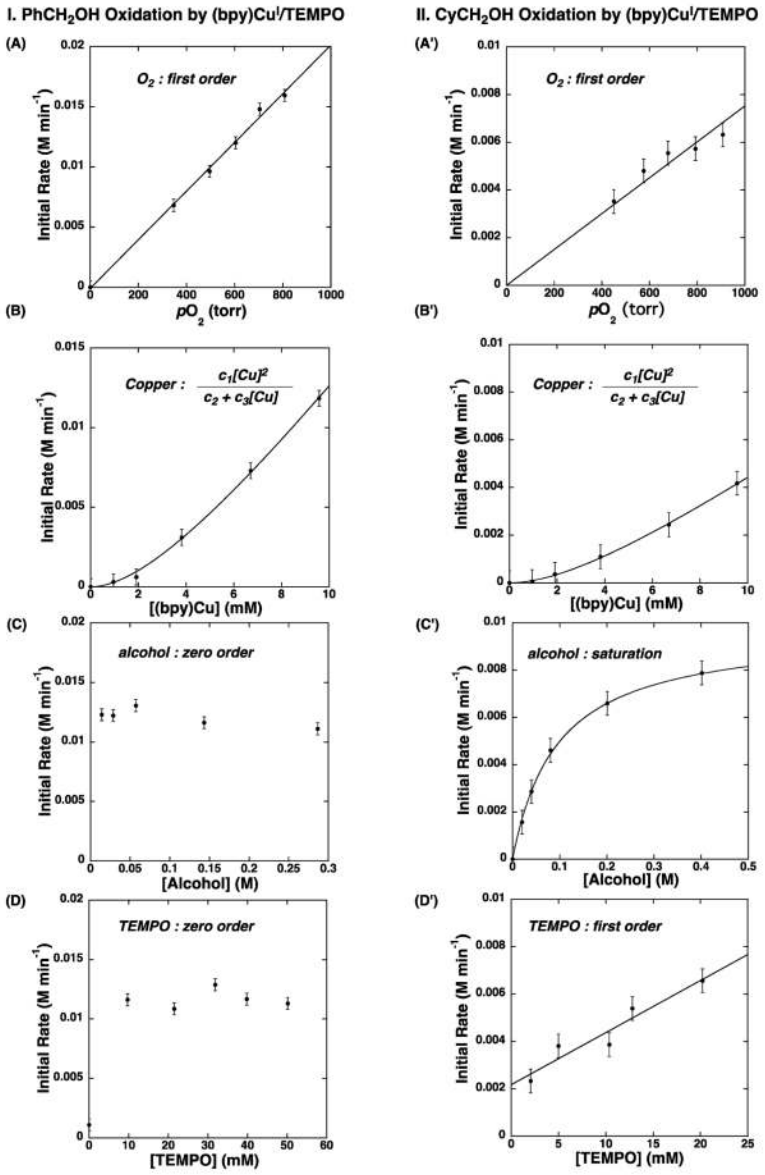


**Figure 7.**

Kinetic data from the oxidation of $PhCH_2OH$ and $CyCH_2OH$ by (bpy)$Cu^{I}$(OTf)/TEMPO assessing the kinetic dependence on (A) $pO_2$, (B) [(bpy)Cu], (C) [alcohol], and (D) [TEMPO]. Rates were obtained by monitoring pressure changes during catalytic turnover. Standard reaction conditions: 10 mM (bpy)Cu, 10 mM TEMPO, 20 mM NMI, 0.2 M $RCH_2OH$, 2.5 mL MeCN, 600 Torr $O_2$, 27 °C. The curves in (B) are derived from a nonlinear least-squares fit to rate = $c_1[Cu]^2/(c_2 + c_3[Cu])$. The curve fit in plot C reflects a nonlinear least-squares fit to rate = $c_1$[alcohol]/ ($c_2 + c_3$[alcohol]). Gas uptake traces are included in Supporting Information (Figures S7–S14).

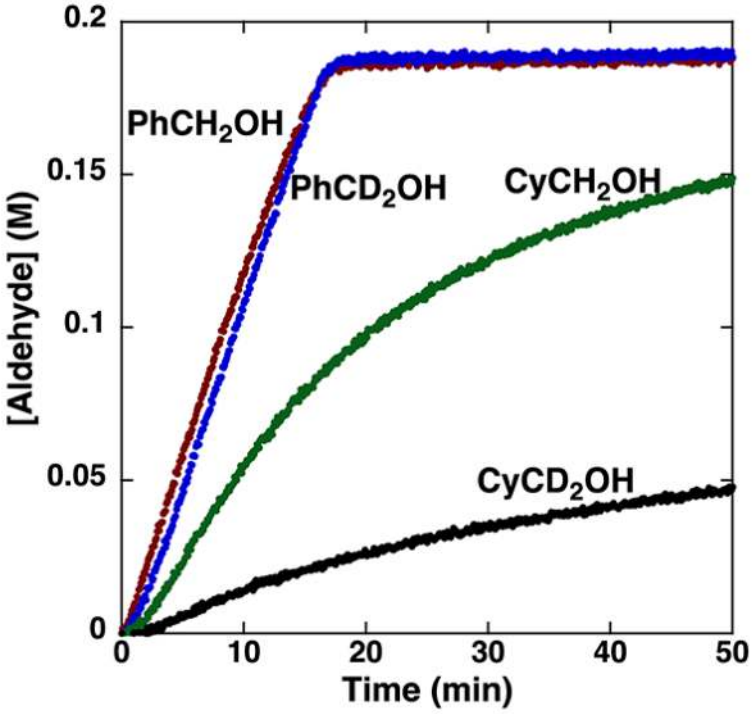


**Figure 8.**

Kinetic profiles for the oxidation of $PhCH_2OH$ (purple), $PhCD_2OH$ (blue), $CyCH_2OH$ (green), $CyCD_2OH$ (black), by $Cu^{I}$(OTf)/TEMPO. Rates were obtained by monitoring gas uptake during catalytic turnover. Standard reaction conditions: 10 mM (bpy)Cu, 10 mM TEMPO, 20 mM NMI, 2.5 mL MeCN, 600 Torr $O_2$, 27 °C.

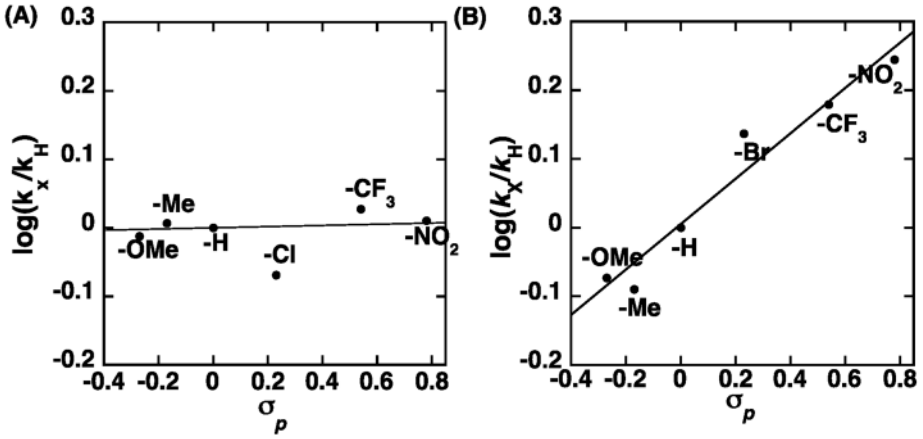


**Figure 9.**

Hammett plots reffecting (A) comparison of independent rate measurements of *para*-substituted benzyl alcohols and (B) competition experiments involving *para*-substituted benzyl alcohols. Rates were obtained by monitoring gas-uptake and analyzed according to the method of initial rates for (A). For (B), product ratios were determined by $^{1}$H NMR spectroscopy at early conversion. See Figure 2 for reaction conditions.

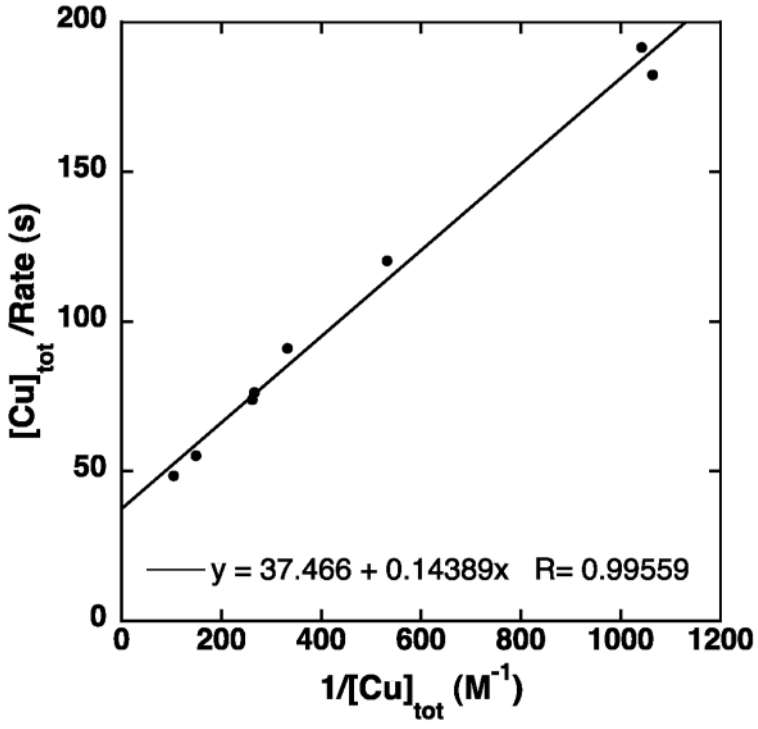


**Figure 10.**
Double reciprocal plot of the [(bpy)Cu] dependence.

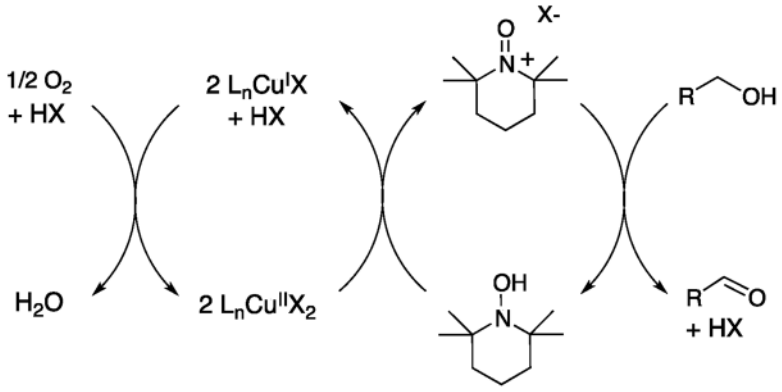


**Scheme 1.**
Oxoammonium-Based Oxidation Pathway

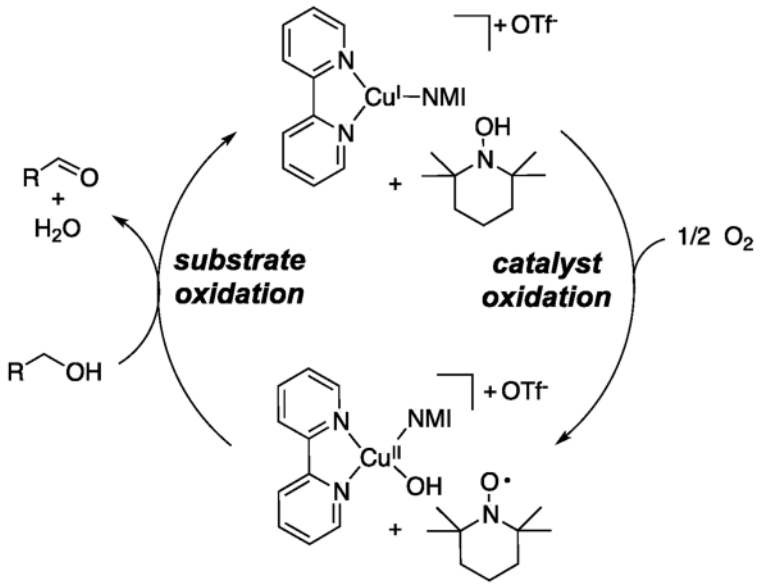


**Scheme 2.**
Simplified Catalytic Cycle for (bpy)$Cu^{I}$/TEMPO Catalyzed Aerobic Alcohol Oxidation

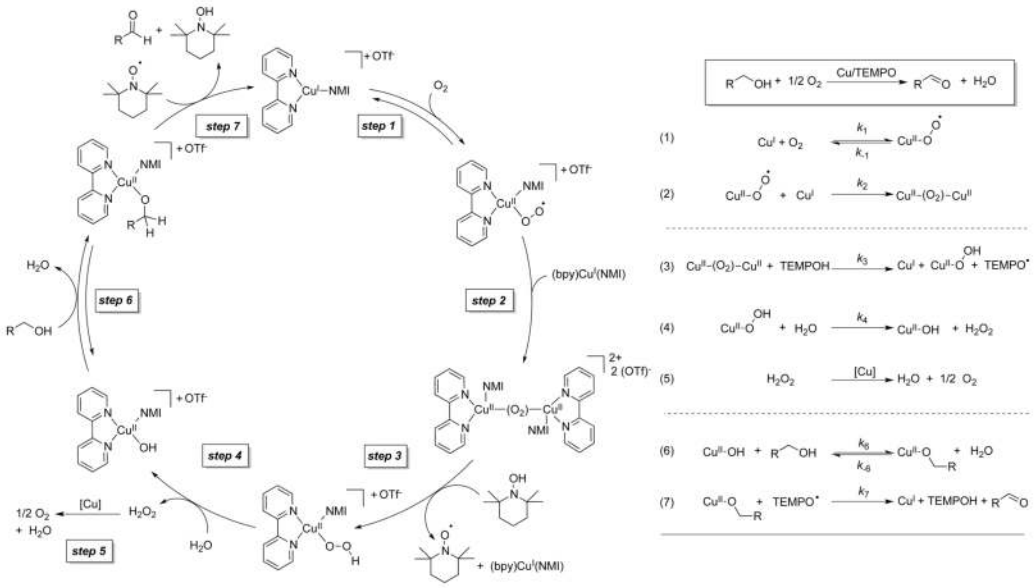


**Scheme 3.**
Proposed Catalytic Cycle for $Cu^{I}$/TEMPO Catalyzed Aerobic Alcohol Oxidation

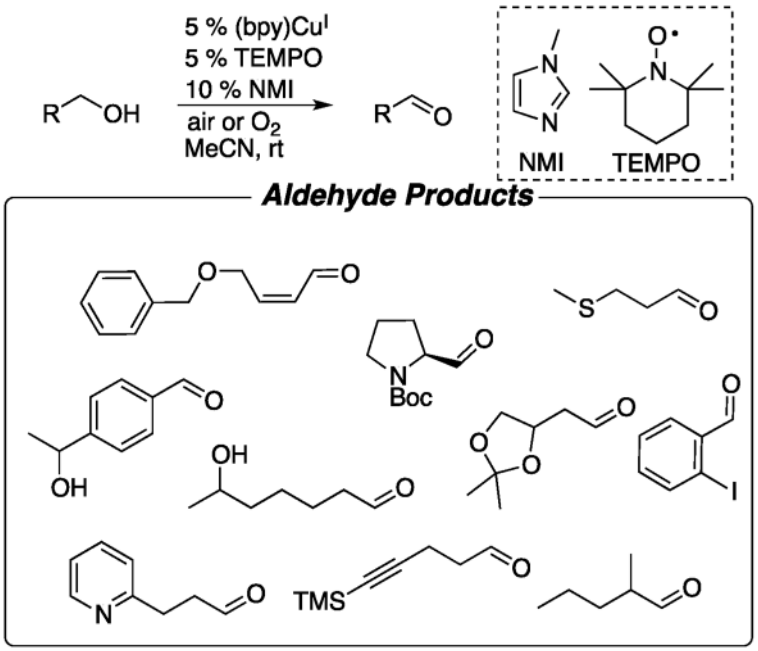


**Chart 1.**
Representative Substrate Scope for (bpy)Cu$^{I}$/ TEMPO/NMI Alcohol Oxidation System

## Table 1

Kinetic Isotope Effects for (bpy)$Cu^{I}$/TEMPO Catalyzed Alcohol Oxidations[a]

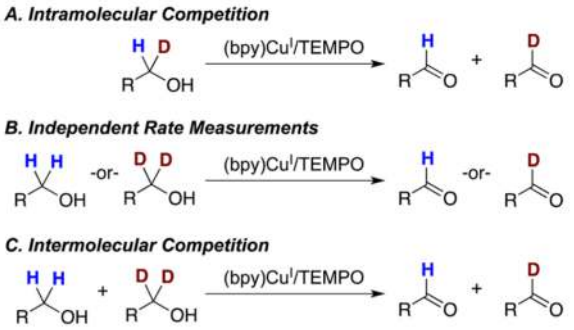


| Experiment | R=Ph | R=Cy |
|---|---|---|
| A. Intramolecular Competition | 6.06(4) | 10.9(9) |
| B. Independent Rates | 1.05(1) | 3.5(1) |
| C. Intermolecular Competition | 2.01(18) | 2.20(16) |

[a]Reaction conditions: 10 mM (bpy)Cu, 20 mM NMI, 10 mM TEMPO, 0.2 M alcohol, 2.5 mL MeCN, 27 °C. For KIE values with $TEMPO^{+}$ see reference 30.